IAC-18- D2.6.3

Aerodynamic Studies in Preparation for CALLISTO - Reusable VTVL Launcher First Stage Demonstrator

J. Klevanski[a]*, T. Ecker[b], J. Riehmer[a], B. Reimann[c], E. Dumont[d], C. Chavagnac[e]

[a] *Department of Supersonic and Hypersonic Technology, Institute of Aerodynamics and Flow Technology, German Aerospace Center (DLR), Linder Höhe, 51147 Cologne, Germany*
[b] *Department of Spacecraft, Institute of Aerodynamics and Flow Technology, German Aerospace Center (DLR), Bunsenstraße 10, 37073 Gottingen, Germany*
[c] *Department of Spacecraft, Institute of Aerodynamics and Flow Technology, German Aerospace Center (DLR), Lilienthalplatz 7, 38108 Braunschweig, Germany*
[d] *Department of Space Launcher Systems Analysis (SART), Institute of Space Systems, German Aerospace Center (DLR), Robert Hooke Straße 7, 28359 Bremen, Germany*
[e] *CNES Launcher Directorate, 52 rue Jacques Hillairet 75612 Paris, France*
**Josef.Klevanski@dlr.de*

Abstract

Reusability applied to launchers is expected to reduce costs of access to space and increase of the operational flexibility. With the goal to improve knowledge in this field, DLR, CNES and JAXA are jointly developing a vertical take-off and landing (VTVL) reusable and scaled launcher first stage demonstrator. With this vehicle, called CALLISTO (Cooperative Action Leading to Launcher Innovation in Stage Toss-back Operations), DLR, CNES and JAXA want to acquire and demonstrate the capability to recover and reuse a vehicle under conditions representative for an operational launcher first stage. Furthermore, during CALLISTO flights, data will be gathered to improve knowledge on the operation of reusable vehicle and therefore help optimizing reusability capabilities of future launch systems.

In order to demonstrate the feasibility of the CALLISTO project during the system requirement review (SRR) and in preparation of the Preliminary Design Review (PDR), extensive aerodynamic analyses have been performed. The entire CALLISTO reference mission is complex and includes many flight phases: ascent, tilt-over manoeuvre, descent and landing. During the flight, the vehicle aerodynamic configuration, the mass, the centre of gravity position and the inertia characteristics change significantly. The flight envelope is characterised by a large range of Mach numbers and dynamic pressures, the angle of attack changes from 0° during ascent to 180° during descent and landing. One of the most important flight phases is the controlled descent through the dense layers of the atmosphere with aerodynamic control surfaces. Therefore aerodynamic design of the vehicle and especially guarantying stability and controllability are of key importance.

The use of classic engineering aero-prediction methods cannot provide the necessary precision and reliability for the estimation of the aerodynamic coefficients even in very early design phase. Therefore CFD methods have to be used even in very early design processes.

For instance, the simulation of the retro-propulsion plume is of particular importance, as it has a major impact on base pressure distribution and aerothermal loads. The paper summarises the main findings of the aerodynamic analysis and show the progress made up to now for CALLISTO project.

Keywords: CALLISTO, aerodynamic, reusability, toss-back, vertical landing, VTVL, CFD, re-entry

Nomenclature

C_D	Drag coefficient	-	C_p	Pressure coefficient	-
C_L	Lift coefficient	-	Ma	Mach number	-
C_m	Pitching moment coefficient	-	Re	Reynolds number	-
C_A	Axial force coefficient	-	q_{dyn}	Dynamic pressure	Pa
C_N	Normal force coefficient	-			

Acronyms/Abbreviations

AEDB	Aerodynamic Database
ALS	Approach & Landing System
ATDB	Aerothermal Database
AoA	Angle of Attack
CALLISTO	Cooperative Action Leading to Launcher Innovation in Stage Toss-back Operations
CFD	Computational Fluid Dynamics
CNES	Centre National d'Etudes Spatiales: French Aerospace Centre
DLR	Deutsches Zentrum für Luft- und Raumfahrt: German Aerospace Center
JAXA	Japan Aerospace Exploration Agency
LH2	Liquid Hydrogen
LOx	Liquid Oxygen
MEIG	Main Engine Ignition
MECO	Main Engine Cut-Off
PTO	Powered Tilt-Over Manoeuvre
RCS	Reaction Control System
RLV	Reusable Launch Vehicle
SRR	System Requirement Review
TVC	Thrust Vector Control
VTVL	Vertical Take-Off and Landing
WTT	Wind Tunnel Test

Note that vehicle configuration naming is explained in Table 1.

1. Introduction

The main goals of the implementation of reusability are to reduce the costs of access to space, and to increase the operation flexibility of launch vehicles. The reuse of elements of launch vehicles has been the object of many research projects and studies in the past. The success reached in the recent years by Space X [1], [10], [13], [17] and Blue Origin [2] in the reuse of the elements of space transportation systems based on the VTVL-concept initiated a renewed interest for RLV research activities.

Facing this reusability challenge for future launchers, DLR and CNES have settled a common and ambitious work-plan addressing the different aspects of this challenge, shared with ArianeGroup and ESA.

One of the challenges in this work plan is the development of the low-cost and reusable engine PROMETHEUS demonstration, featuring LOx and methane propellants and for which firing tests are planned in 2020.

In parallel, a set of flying demonstrations are in preparation, based on DLR and CNES background and past studies, covering system aspects of both vertical and horizontal landing modes.

In terms horizontal landing winged first stages, ReFEx is a technology demonstration at DLR and will fly in 2021 see [14] for more details. In addition, FALCon (Formation flight for in-Air Launcher 1st stage Capturing demonstration) is an elementary demonstration, aiding in the complete system analysis options for winged first stages, dedicated to in-air capturing technology.

In terms of vertical landing, following the EAGLE (DLR) [5] and FROG (CNES) "sandbox" experiences, the medium scale CALLISTO (Cooperative Action Leading to Launcher Innovation in Stage Toss-back Operations) [4], [7] and [18] is the next step demonstration, conducted as a tri-lateral project between CNES, DLR and JAXA and is planned to be flown in 2022.

The last step will be the yet to be defined THEMIS real-scale demonstration featuring PROMETHEUS engine and using experiences and system studies based on the previous and aforementioned flight experiments. This set of demonstrations will help in deciding on the right choice for European future operational launchers.

One decisive step in this roadmap is the experimental reusable VTVL demonstrator CALLISTO. This scaled vehicle is dedicated to the demonstration of the capability to recover and reuse a vehicle under conditions representative of a future operational launcher. This research project will allow developing, improving and testing the key technologies and knowledge necessary for the implementation of reusability. The related experience will be gathered in the course of several flights performed with the same vehicle.

The CALLISTO demonstrator is based on an existing LOx/LH2 reusable and re-ignitable rocket engine provided by JAXA. The thrust level is about 40 kN with a large range of continuous throttling capability.

2. Mission Analysis and Flight Configurations

The primary mission objective is to demonstrate a so-called "toss-back" flight profile, which includes in particular:

- classic ascent phase (when compared to an expendable launch vehicle
- attitude change phase, called "tilt-over"-manoeuvre
- "boost-back" phase with targeting the landing site
- aerodynamic guided approach phase
- final landing boost and touchdown

In fact, on top of this reference flight profile, several flight profiles are under investigation in order to establish a consistent flight test plan which would enable to incrementally increase the difficulty of the flight until the reference flight profile.

A candidate trajectory is shown in Fig. 1.

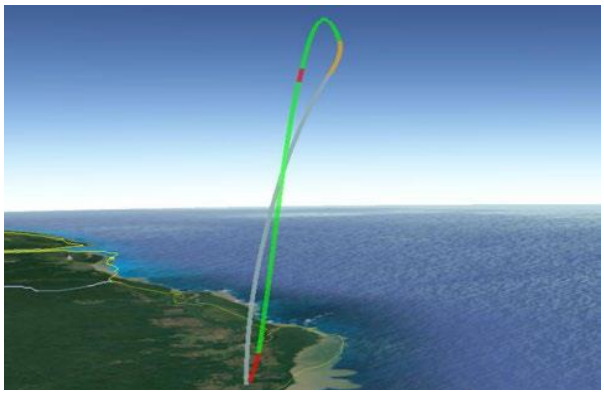

Fig. 1. Candidate trajectory.

The use of only one motor is very challenging: acceptable thrust to weight ratio should be provided for the start as well as for landing. It is much more difficult in comparison with launchers with many rocket engines like for example Falcon 9 with 9 motors. The available engine thrust with the 40% throttling ratio limits the start mass as well as the landing mass.

According to different limitations, the dynamic pressure along the trajectory is relatively high – too high in some cases to perform a tilt-over manoeuvre relying on RCS (reaction and control system) thrusters only. As alternative, the tilt-over-manoeuvre can be also performed by deflection of the main engine with TVC while the engine is still running. This kind of manoeuvre was called "powered tilt-over" manoeuvre (PTO). Preliminary analyses show that under certain conditions a PTO results in better performance. Impacts to and adaptations of resulting flight phases are under investigation.

Then the aerodynamic design of CALLISTO has to be very extensive: Mach number, altitude and dynamic pressure vary in a very broad range, the vehicle flies forwards in the ascent phase and rearwards in the approach and landing phases, during the tilt-over manoeuvre the angle of attack varies from 0 to 180°. Furthermore, the flight configuration changes for each flight phase: the aerodynamic control surfaces (fins) and landing legs are stowed during the ascent phase, the fins are then deployed for the aerodynamic descent / approach phase. Finally, the landing legs are deployed shortly before the touch-down.

The nomenclature of the flight configurations used in accordance with the flight phases is given in Table 1. Note that aerodynamic characteristics of the vehicle on the launch pad before launch is also the object of CFD computations (not presented here) influencing the design of the CALLISTO system.

Table 1. CALLISTO flight configurations.

Configuration		Phase Applicable	Fins	Landing Legs	Thrust Plume
FFO (C0)		Ascent and Powered Tilt-Over: MEIG#1 – MECO#1	Folded	Folded	Thrust Plume
FFN (C1)		Ballistic MECO#1 – Fin Deploy	Folded	Folded	No Thrust Plume
UFN (C2)		Ballistic: Fin Deploy – MEIG#2 *and* Aerodynamic Descent: MECO#2 – MEIG#3	Unfolded (Deployed)	Folded	No Thrust Plume
UFO (C3)		Brake Boost: MEIG#2 – MECO#2 *and* Approach Boost: MEIG#3 – Legs Deploy	Unfolded (Deployed)	Folded	Thrust Plume
UUO (C4)		Landing: Legs Deploy – MECO#3	Unfolded (Deployed)	Unfolded (Deployed)	Thrust Plume + Ground Effect
UUN (C5)		Landed (Park): After MECO#3	Unfolded (Deployed)	Unfolded (Deployed)	No Thrust Plume + Wind Stability

The trajectory was analysed to indicate the flight phases and configurations which are particularly important from an aerodynamic point of view. For each flight phase and configuration the relative forces were compared: aerodynamic forces, thrust and RCS-forces.

The results are shown in Fig. 2. It can be seen that from aerodynamic point of view, the most important phase is the aerodynamically controlled descent, in other words the flight configuration UFN (C2).

The configuration C1 is not as critical as in this case the weight is largely dominating, but it shows the limitation of the RCS capabilities.

Both configurations UFN (C2) and UFO (C3) requires knowledge of the whole range of AoA = 0° to +180°.

In the case of configuration FFO (C0) and FFN (C1) knowledge of aerodynamic characteristics and especially the drag is important for small angle of attack (AoA), in the range: -5° - +5°.

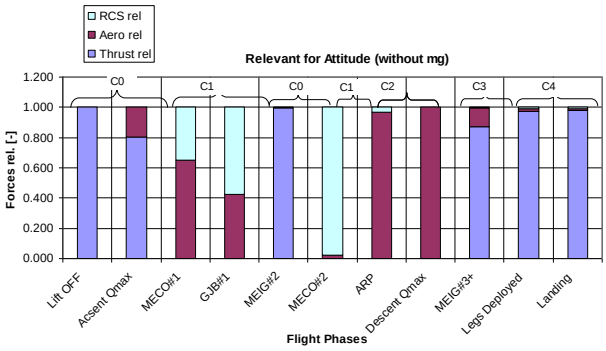

Fig. 2. Comparison of forces order of magnitude for relevant configurations and flight points.

Nevertheless for the dynamic simulation of the tilt-over manoeuvre the complete circular polar should be calculated for the AoA = -180° to +180°, in the case of configuration FFO (C0).

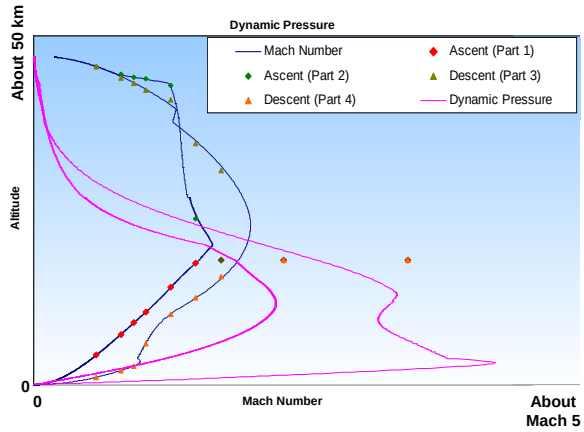

Fig. 3. Possible flight profile: Ma, q_{dyn} = f (H).

The calculation matrix was defined on basis of one of the possible flight profile shown in Fig. 3. In order to avoid extrapolation, higher Mach numbers were also simulated with a constant altitude.

3. Evolution of Aerodynamic Shape

Different vehicle layouts have been considered and analysed in the preliminary design phase. The development of the CALLISTO aerodynamic shape was accomplished with intensive aerodynamic studies: each layout was checked by extensive CFD calculations performed with so called "Low Resolution Euler" simulation (see chapter 6).

One of the most critical design parameters is the vehicle diameter. On the one hand, the chosen diameter should provide the acceptable slenderness (length-to-diameter ratio) to minimize the aerodynamic drag, on the other hand, it should be sufficiently wide to accommodate the different subsystems.

In the early phases of the design different vehicle layouts have been considered with special emphasis on core diameter of the vehicle and its impact to vehicle length and carrying structure main sizes. For the different diameters concepts with extended aft bay and/or boat tail have been studied as well.

Fig. 4 and Fig. 5 show clearly that an extended aft bay results in a dramatic increase of aerodynamic drag especially for transonic and supersonic speeds. The boat tail shape is allowing reducing strongly the drag for subsonic regime in the case of a vehicle with extended aft-bay. The drag level is then comparable to the one of a vehicle without extended aft-bay. The core diameter of the vehicle has limited influence on the drag at 0° angle of attack, if a larger extended bay is used. What counts is whether an extended bay (i.e. with a large diameter) or a boat tail is used. Basically the maximum cross section area influences the drag in trans- and supersonic regimes. The base area is determining the drag level at subsonic speeds. The choice of the diameter was partially linked to landing legs. If the aft bay is too short, it is difficult to combine it with landing legs. The aerodynamic analysis showed that the best solution was keeping the straight layout of CALLISTO (non-varying core diameter) and no extended aft bay.

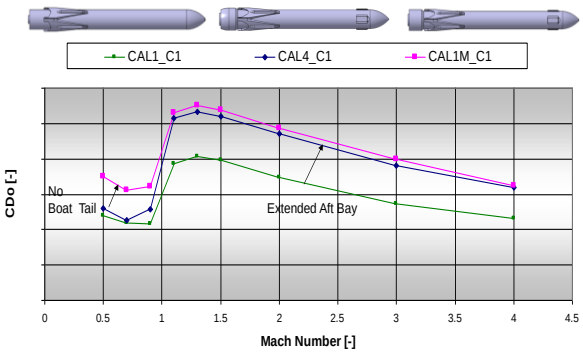

Fig. 4. Aerodynamic shape variation and impact of boat tail and extended aft bay

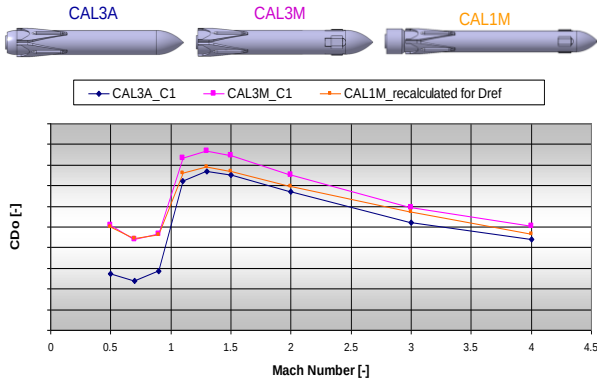

Fig. 5. Aerodynamic shape variation and impact of vehicle diameter and boat-tail

The definition of the kind and shape of the aerodynamic control surfaces were the next important decision. One of the first design variants considered in the early design phase were the grid fins, for which DLR has a significant background and published patents [15].

The known advantages of grid fins in comparison to plain fins are the compact design and smaller hinge moments. In the current stage of the project the reference design considers plain fins which show more predictable behaviour in the transonic regime. The comparative study with grid fins is still on going.

A proposed option featuring deployed fixed fins during the whole flight was investigated. The study showed that wind gust during ascent would result in

stability loss and therefore a mechanism to stow fins during ascent is a must.

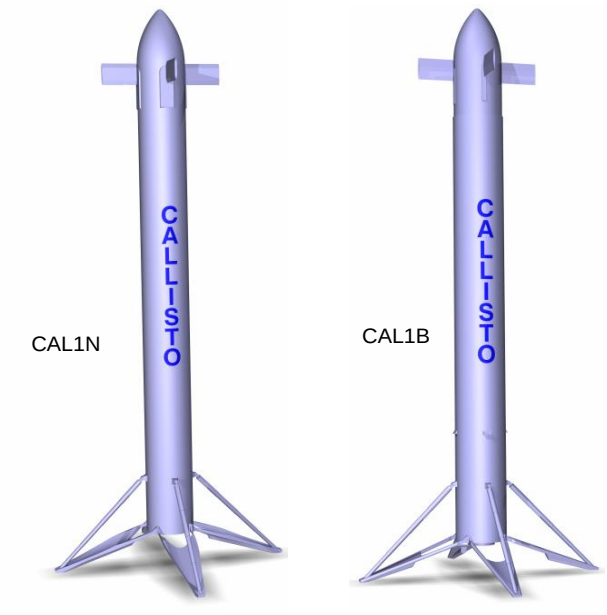

Fig. 6. Aerodynamic shapes CAL1N and CAL1B.

The fin size was defined to provide the natural (not artificial) static stability of the vehicle during the aerodynamic descent phase for the UFN (C2) configuration with respect to the expected centre of gravity according to the requirements. The fin size was chosen to provide the natural stability for the expected CoG position and AoA range during the descent phase.

The aerodynamic shape called CAL1N was the result of the vehicle layout evolution. This layout was the base line during the System Requirement Review (SRR). Further improvements lead to relative small modifications in the layout e.g. fin profile choice and landing legs optimisation.

These improvements were included in the modified layout for the design phase B0 called CAL1B (Fig. 6).

4. Applied Methods and Creation of AEDB / ATDB

The philosophy and strategy of the aerodynamic study is presented in Fig. 7 in the form of a "road-map".

The aerodynamic calculations performed during the design phases A and B0 were:

- Aerodynamic design, including body shape optimization and fin sizing, analysis of trimmability, stability & controllability
- Calculation of aerodynamic coefficients for AEDB
- Calculation of distributed loads and fin loads for further structure analysis

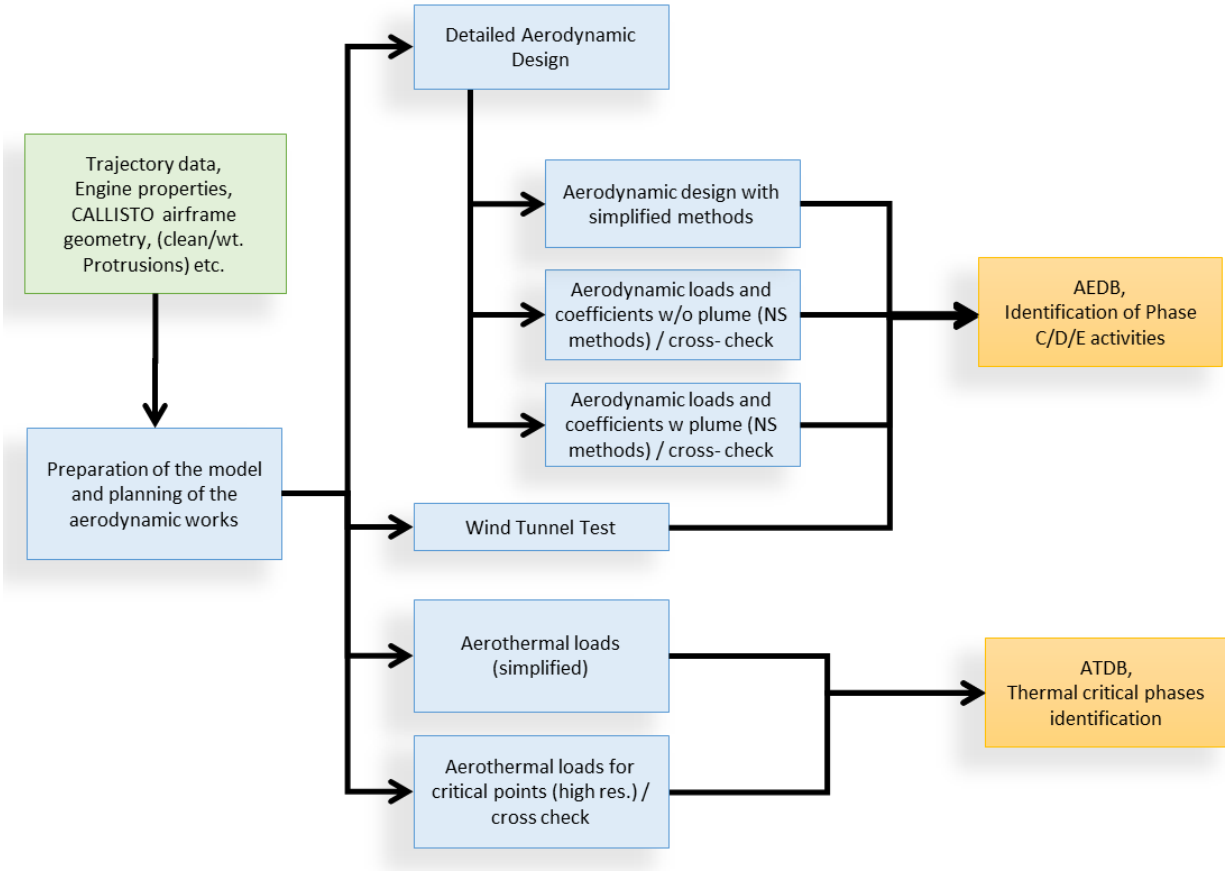

Fig. 7. "Roadmap" for aerodynamic and aerothermodynamic studies.

- Calculation of aerothermal loads
- Study and optimisation of the fin profile

A simplified method and a high fidelity method were combined for the synthesis of the AEDB. The special features and application of these methods are shortly described below.

4.1 Preliminary Aerodynamic Design Methods

The concept study during the preliminary design phase is important for the successful definition of the vehicle layout. Many aerodynamic computations should be performed in a short period of time with limited computational resources, in order to assess a large number of layouts. The so called "aero-prediction" codes, e.g., calculation methods like Missile DATCOM [19] can usually successfully be used for the preliminary design of missiles and launchers. These methods are very fast and the preparation of the input data is relatively easy. These methods are very efficient for choosing the main design parameters (fuselage diameter, fin size etc.).

However, the analysis of the CALLISTO special features mentioned in the chapter 2 (wide range of Mach numbers, AoA = 0° to 360°, several flight configurations, "ejector"-effect of engine etc.) shows, that the domain of the successful application is strongly restricted for the typical aero-prediction codes like Missile DATCOM. These codes are well suited for the calculation of the aerodynamic coefficients for launchers or missiles (typically simple revolution bodies) and for a limited range of the angle of attack. They are not well suited for complex aerodynamic shapes. The superposition principles used in these codes will not allow the precise calculation of the fin/fuselage interaction and the calculation of the distributed forces.

Therefore CFD methods were applied already in the concept design phase: CFD allows the aerodynamic calculations for subsonic as well as for transonic and supersonic; for both simple and complex shapes.

The CFD solver TAU (developed in DLR [11], see 4.2) was used already for the preliminary aerodynamic design. The aerodynamic domain mesh was generated for each of the flight configurations identified in the computation matrix and for five reference fin deflections of -20°,-10°, 0°, +10°, and +20°.

Usually CFD methods require large amount of computational resources. In order to reduce the calculation time for the "Low-Resolution" Euler method the CFD solver used a coarse mesh, frictionless flow with Euler wall boundary conditions. The symmetry of vehicle allowed the use of half-body mesh domain in the majority of calculations – the full-body domain was only used for the calculation of the roll moments. This way the calculation time could be reduced to several minutes per configuration and case (set of flow parameters).

All the meshes were generated with the CENTAUR mesh generator [3] based on water-tight aerodynamic shapes (Fig. 8). The same shapes were used also for the high fidelity aerodynamic computations (see section 4.2) in order to combine the results.

A two-gas mixture approach was used for the engine plume simulation (without simulation of chemical reactions). Using standard air for the outer flow and an exhaust gas based on the products of the hydrogen-oxygen combustion.

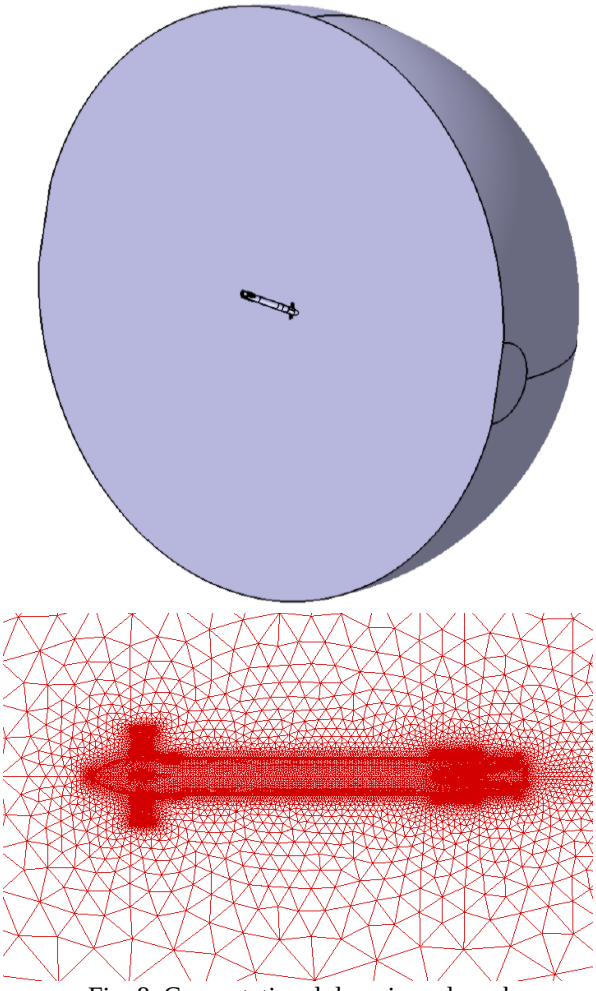

Fig. 8. Computational domain and mesh.

4.2 High Fidelity Aerodynamic Calculation.

All high fidelity numerical investigations for the aerodynamic and aero-thermal analysis of both ascent and descent were performed using the hybrid structured/unstructured DLR Navier-Stokes solver TAU. This DLR developed solver is validated for a wide range of steady and unsteady sub-, trans-, super-, and hypersonic flow cases. The TAU code is a second order finite-volume solver for the Euler and Navier-

Stokes equations in the integral form using eddy-viscosity, Reynolds-stress or detached and large eddy simulation for turbulence modelling. For the presented investigations, the Spalart-Allmaras one-equation eddy viscosity model [16] was used. The AUSMDV flux vector splitting scheme was applied together with MUSCL gradient reconstruction to achieve second order spatial accuracy. The applied model for thermodynamic and transport properties are based on a non-reacting mixture of thermally perfect gases (air and engine exhaust) and are derived from the CEA thermodynamic and transport databases.

Detailed aerodynamic design performed by means of the high fidelity methods include:

- Calculation of the aerodynamic coefficients with the high fidelity tools (CFD: TAU Euler and Navier-Stokes etc.)
- Analysis of the aerodynamic flow for critical cases (including in particular plume effects during ascent, and retro-boosts)
- Analysis and verification of the calculated aerodynamic coefficients
- Evaluation of uncertainties
- Recommendations to vehicle on the aerodynamic and shape design
- Determination of pressure distribution
- 2D and 3D calculations of the aerothermal loads during the CALLISTO trajectory
- Analysis of the aerothermal loads for critical cases (including in particular plume effects during ascent, and retro-boosts)
- Determination of heat flux distribution on specified thermal interfaces

4.3 Main Results and Synthesis of the AEDB

All preliminary calculations of the aerodynamic coefficients were performed by means of CFD methods "Low-Resolution" in Euler mode. These calculations provided the results in the short time by use of the limited computational capabilities. The time necessary for computation for all configurations for a reference shape is 3-4 weeks on a typical workstation. However, the cross-check with the results gained by means of the high fidelity Navier-Stokes methods showed, that the adequate accuracy cannot be reached only with the low resolution methods, especially for subsonic flow.

The Navier-Stokes calculations provide the necessary accuracy but they require a large amount of computational resources and calculation time. For the most important configurations and flight regimes (ascent configuration FFO for AoA = ±10° and aerodynamically controlled descent configuration UFN, AoA = ±170°) the aerodynamic coefficients were calculated by use of the high fidelity Navier-Stokes methods. The final data basis was built as a synthesis by combining both results of the "Low-Resolution" Euler and the high fidelity results as explained below.

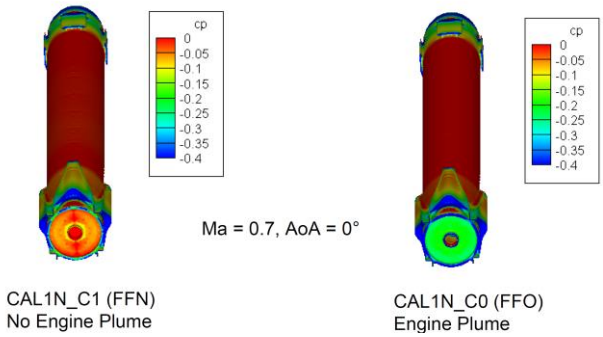

Fig. 9. Ejector effect: base pressure influence.

One of the aerodynamic effects with strong impact on the CALLISTO performances is the so-called "ejector-effect". Ejector effect appears as the drag increase due to the influence of the low pressure region on the base surface of the vehicle caused by engine jet.

Ejector effect depends strongly on the engine jet (plume) expansion e.g. on the environment pressure at the flight altitude (Fig. 9, Fig. 10). For CALLISTO the ejector effect is very dominant due to the large ratio between nozzle exit diameter and vehicle diameter.

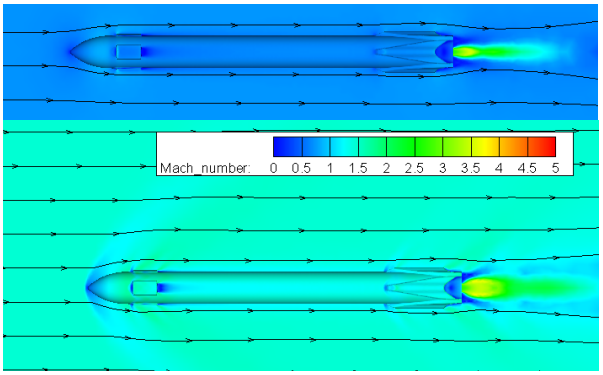

Fig. 10. Plume expansion influence.

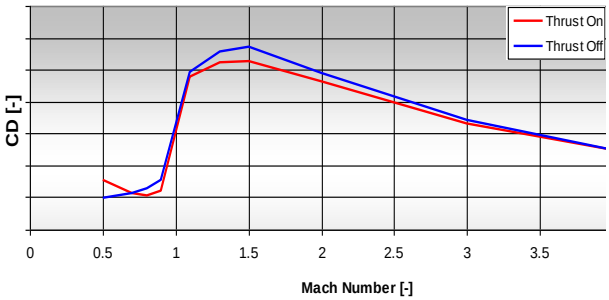

Fig. 11. Drag coefficient C_D for ascent phase and impact of ejector effect

The "Low-Resolution" Euler-method over predicts the ejector effect resulting in a higher drag coefficient in

subsonic. The results should be corrected in accordance with the more precise "high resolution" Navier-Stokes-calculation by introducing of a correction coefficients (Fig. 11).

The correction factor F_{cor} was determined for each Mach number based on the comparison of the "Low-Resolution" Euler results with the Navier-Stokes results calculated for FFO (C0) configuration at AoA = 0°.

$$F_{cor}(Ma) = \frac{CDo_{NS}(Ma, \alpha = 0)}{CDo_{EUL}(Ma, \alpha = 0)} \quad (1)$$

The full correction factor F_{cor} is applied for AoA = 0° and will gradually change to 1 (no correction) for AoA ≥ 90° (see Eq. (2) and Fig. 12). As it can be seen the strongest correction is applied to subsonic and transonic flow conditions.

$$F_{cor}(Ma, \alpha) = 1 + (F_{cor}(Ma) - 1) \cdot \cos(\min(\alpha; 90°)) \quad (2)$$

The calculation of the aerodynamic coefficient results in the estimation of the flight qualities. They play an important role in particular for the aerodynamically controlled descent, for instance on the vehicle stability (see Fig. 13.) Uncertainties on the aerodynamic coefficients and therefore on the flight qualities have a large impact on the reachable flight envelope and require an extra attention.

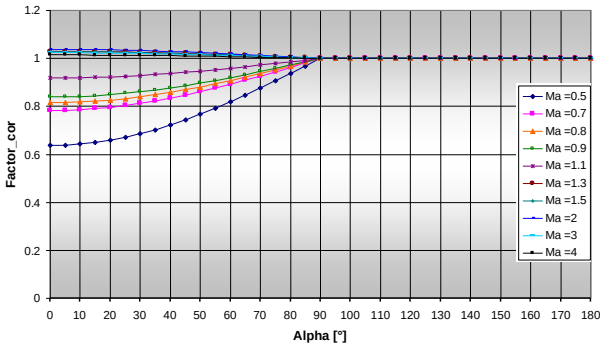

Fig. 12. Correction factor versus angle of attack.

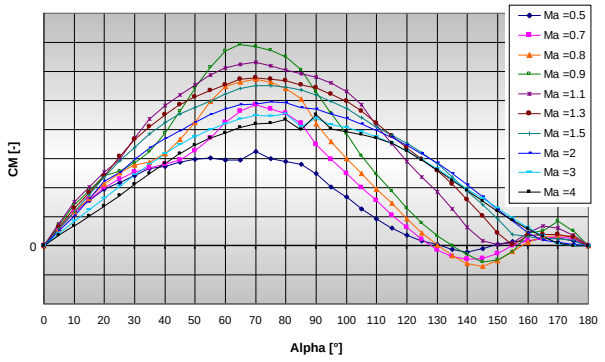

Fig. 13. Pitching moment coefficient C_m over Mach number and angle of attack.

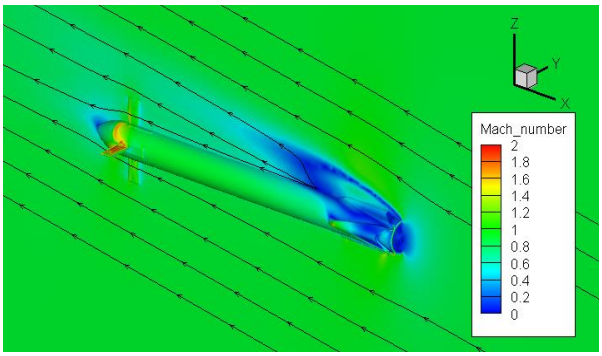

Fig. 14. Flow field during non-propelled descent (AoA = 170°, Ma = 0.9).

An example of CFD results for the aerodynamically controlled part of the descent is shown in Fig. 14. During the propelled part of the flight the thrust is usually much larger than the aerodynamic force reducing the influence of aerodynamic uncertainties. The propelled part of the descent is an extreme case, as the modification of the flow around the vehicle by the exhaust gases decreases the aerodynamic drag to nearly zero.

4.4 Planed Wind Tunnel Tests

In order to confirm the CFD analysis, wind tunnel tests (WTT) are already in preparation. They will include the most critical configurations for both ascent and descent flight phases. The modular models for the WTT are based on the watertight aerodynamic shape CAL1B defined for the design phase B0. The first part of the wind tunnel tests will be performed in the Trisonic Wind Tunnel TMK-facility in Cologne. The TMK allows to operate in the range of Mach number Ma = 0.5 to 5.7 with wide Reynolds number variation. The WTT experiments include:

- Aerodynamic measurement: forces, moments
- Schlieren imaging
- Oil flow pictures
- Ma = 0.5 to 3.0
- AoA = -20° to +20°; 160° to 200°
- Configurations: FFN (C1) and UFN (C2)

5. **Aerothermal Aspects**

The aerothermal aspects of the CALLISTO vehicle are a critical field of study. One of the key differences between a reusable full size launcher like Falcon 9 and CALLISTO is the relatively low Mach number during the descent. This means that aerodynamic heating during the trajectory is minimal and almost all design driving thermal loads are due to the hot exhaust plume during the retro boost. Other potential thermal loads are due to plume-ground interaction, as well as radiation

from the hot landing pad surface. For the purpose of phase A, several possible configurations were investigated using CFD methods [7].

5.1 Aerothermal aspects of shape development

The heat flux and flow field temperature for a reference trajectory point for three of the considered configurations of phase A is shown in Fig. 15.

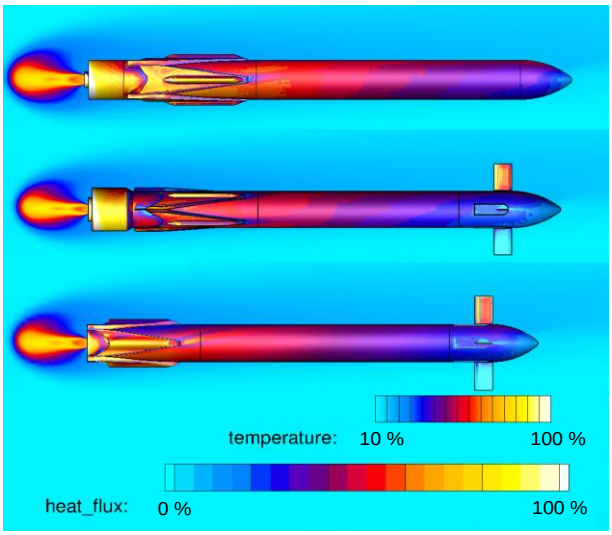

Fig. 15. Relative heat flux and gas temperature during propulsive re-entry phase for three of the considered configurations. (AoA = 175°, Ma = 0.7) during phase A previously presented by [7].

As can be seen, the highest heat fluxes are mainly due to heating from hot exhaust gases and heated air in proximity of the aft bay and on the exposed structures like legs and fins. Moving the legs closer to the tail during the design process of phase A resulted in a beneficial impact on the thermal loads on the lower part of the vehicle.

The development of the plume extension is different for the considered re-entry, when compared to Falcon 9, or the studies presented in [6] and [9]. As shown by Dumont et al. [7] the plume remains relatively concentrated at the aft end of the vehicle due to high atmospheric pressure and only very low fractions of actual exhaust gas species enclose the vehicle.

5.2 Low fidelity and high fidelity calculation of aerothermal loads

Current efforts for phase B focus on evaluating the design critical heat fluxes for phase B geometries as well as comparing low and high fidelity aerothermal CFD simulations. Further the loads during touch down and engine shut down are evaluated.

Fig. 16 shows heat flux contours for both re-entry configurations UFO and UUO. While heat fluxes are concentrated mainly on the aft-bay and the legs, the magnitude of heat flux is much higher during the start of the retro-boost manoeuvre compared to the moment the legs are opened for landing.

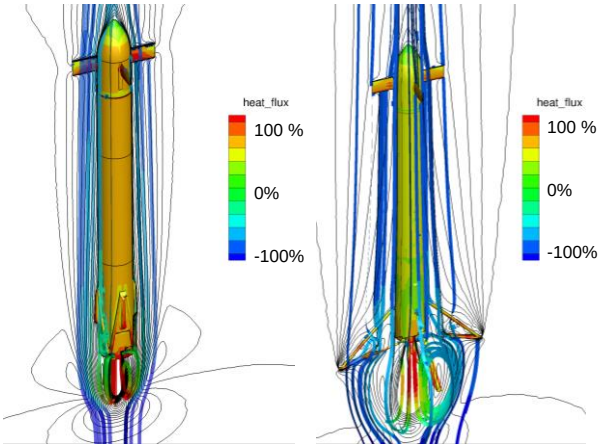

Fig. 16. Relative heat flux during propulsive re-entry phase for configuration CAL1B UFO at M = 0.84 (left) and CAL1B UUO at M = 0.3 (right). Lines represent Mach contours. Ribbons are streamlines coloured by temperature. Scales between figures left and right cannot be compared in magnitude.

The heat flux during engine shut down on landing pad is shown in Fig. 17. A main concern is the dynamic heating of the landing pad and resulting radiation from the pad to the vehicle, as well as hot exhaust gases inflicting damage on the landing legs.

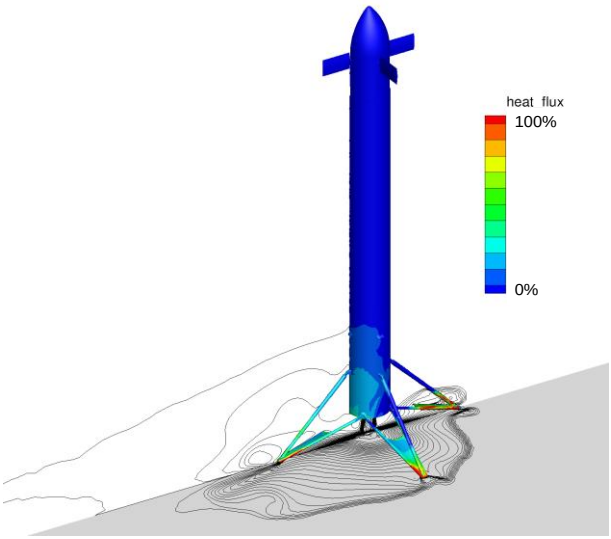

Fig. 17. Relative heat flux during engine shut down on landing pad. Lines represent temperature contours. Simulation includes ground wind velocity of M = 0.1 from the side.

5.3 Main Results and Synthesis of the ATDB

For the aerothermal analysis of the complete trajectory, a multitude of 2D calculations at different

wall temperatures (300 and 400 K) and engine conditions (engine on/off) were conducted. From this data an engineering database with interpolated wall heat fluxes as a function of the wall temperature for the different sections of the vehicle is generated.

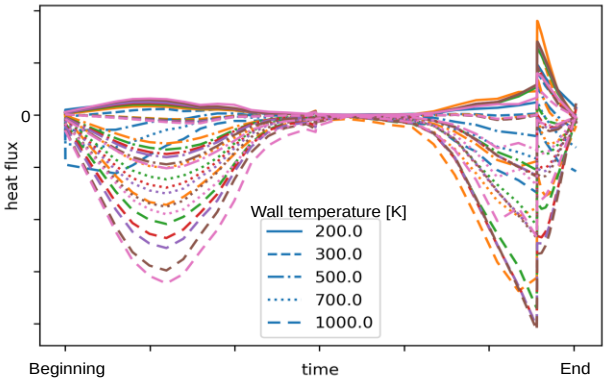

Fig. 18. Heat flux during complete CALLISTO trajectory for configuration CAL1N and different wall temperature.

Fig. 18 shows the heat flux for the trajectory and the different thermal interfaces (fairing, aft-bay, tanks etc.). As can be seen, the retro-boost (step in later part of the time/heat flux diagram) is the major source of heat flux in the vehicle.

At most other times there is no positive heat flux into the vehicle as the wall temperature is likely above total temperature conditions. The application of the linear interpolation method is validated with calculations at higher wall temperatures for a selected range of cases.

6. Conclusion and Outlook

Within the CALLISTO project, DLR, JAXA and CNES are joining their force and experience to develop, build and test a demonstrator of a Vertical Take-off Vertical Landing launch vehicle reusable first stage. CALLISTO, which is part of the CNES and DLR common RLV roadmap and a successor of the RV-X demonstrator of JAXA, is going to demonstrate over the course of several test flights the mastery of the manoeuvres contained within a propulsive return mission.

The aerodynamic design is a very important part of the CALLISTO development. The necessary aerodynamic and aero-thermodynamic data were generated by combining both low resolution and high fidelity CFD methods. The fundamental feasibility of CALLISTO has been shown during the phase A of the project. Phase B which started in March 2018 is on-going. This phase concentrates on the design of the different products. In order to complete and validate the CFD analysis, wind tunnel tests are already in preparation and will take place in late 2018.

Acknowledgements

The authors wish to thank the whole CALLISTO joint project team for the important work performed in the frame of an enriching cooperation.

References

[1] Bhagat M. R., SpaceX Falcon 9 v1.1, Falcon Heavy remodelling; Falcon 9 v1.1 descent trajectory and performance optimization, SART TN-020/2014, 2014.

[2] Blue Origin, https://www.blueorigin.com/new-glenn, as accessed on September 15, 2017.

[3] CentaurSoft, http://www.centaursoft.com

[4] Diaz Lopez, O., Lopez Moreno, S. & Desmariaux, J. (2018), CALLISTO Project – Mechanical Architecture and Structural Design Challenges in the Frame of a Reusable First Stage Demonstration Vehicle, IAC-18.D2.6.4, 69th International Astronautical Congress (IAC), 1-5 October 2018, Bremen, Germany.

[5] Dumke, M., Sagliano, M., Saranrittichai, P., Trigo, G. F. & Theil, S. (2017) EAGLE – Environement for Autonomous GNC Landing Experiments. 10th International ESA Conference on Guidance, Navigation and Control Systems, 29 May - 02 Jun 2017, Salzburg, Austria.

[6] Dumont, E., Stappert, S., Ecker, T., Wilken, J., Karl, S. Krummen, S. & Sippel, M. (2017): Evaluation of Future Ariane Reusable VTVL Booster Stages, IAC-17-D2.4.3, 68th International Astronautical Congress (IAC), 25-29 September 2017, Adelaide, Australia. [http://elib.dlr.de/114430/]

[7] Dumont, E., Ecker, T., Chavagnac, C., Witte, L., Windelberg, J., Klevanski, J. & Giagkozoglou, S. (2018): CALLISTO – Reusable VTVL launcher first stage demonstrator, SP2018_00406, Space Propulsion Conference 2018, 14-18 May 2018, Seville, Spain. [http://elib.dlr.de/119728/]

[8] Ecker, T., Karl, S., Dumont, E., Stappert, S. & Krause, D. (2017) A Numerical Study on the Thermal Loads During a Supersonic Rocket Retro-Propulsion Maneuver. 53nd AIAA/SAE/ASEE Joint Propulsion Conference, 10-12 June 2017, Atlanta, USA. DOI: 10.2514/6.2017-4878 [http://elib.dlr.de/111762/].

[9] Ecker, T., Zilker, F., Dumont, E., Karl, S. & Hannemann, K. (2018) Aerothermal analysis of reusable launcher systems during retro-propulsion Reentry and landing, SP2018_00040, Space Propulsion 2018, Seville, Spain, 14-18 May 2018.

[10] Koch, A., Sippel, M., Kopp, A., van Foreest, A., Ludwig, C. and Schwanekamp, T., Critical analysis of Falcon 1, 1e, Falcon 9 and Dragon capsule, SART TN-018/2010, 2010.

[11] Langer, S. und Schwöppe, A. und Kroll, N. (2014) The DLR Flow Solver TAU - Status and Recent Algorithmic Developments. 52nd Aerospace Sciences Meeting, 13-17 January 2014, National Harbor, Maryland, USA.

[12] Monchaux, D. (2018): FROG, a Rocket for GNC Demonstrations IAC-18-D2.5.3, 69th International Astronautical Congress (IAC), 1-5 October 2018, Bremen, Germany.

[13] Pouplin, J. and Dumont, E. Falcon 9 v1.1 and v1.2 performances and first stage descent/return trajectories analyses, DLR-IB-RY-HB-2016-51, SART TN-009/2015, 2015.

[14] Rickmers, P., Bauer, W., Sippel, M., Stappert, S., Schwarz, R. & Sagliano, M. (2018): An Update of the Upcoming DLR Reusability Flight Experiment – ReFEx, IAC-18-D2.6.1, 69th International Astronautical Congress (IAC), 1-5 October 2018, Bremen, Germany.

[15] Schülein, E, Wing for an Aircraft or Spacecraft, US7114685 (B1), Patent, 2006.

[16] Spalart, P. R., Allmaras, S. R., A One-Equation Turbulence Model for Aerodynamic Flows, AIAA-92-0439, 30th Aerospace Sciences Meeting and Exhibit, Reno, USA, 1992, 6-9 January. DOI: 10.2514/6.1992-439.

[17] Stappert, S. and Dumont, E. Reusability of launcher vehicles by the method of SpaceX, SART TN-007/2016, 2016.

[18] Tatiossian, P., Desmariaux, J. & Garcia M. (2017): CALLISTO Project - Reusable first stage Rocket Demonstrator, DOI: 10.13009/ EUCASS2017-680, 7th European Conference for Aeronautics and Space Sciences, 3-6 July 2017, Milano, Italy.

[19] William B. Blake (1998): Missile DATCOM User's Manual - 1997 FORTRAN 90 Revision. Air Vehicles Directorate, Air Force Research Laboratory, Air Force Materiel Command Wright Patterson Air Force Base, Ohio 45433-7562.